Bioinspired Synthesis of (–)-Hunterine A: Deciphering a Unique Deconstructive Route

Bálint Zsigulics[a,b], Péter Angyal[a,b], Bence Balázs Mészáros[a,b,c], János Daru*[c], Szilárd Varga*[a], Tibor Soós*[a]

[a] B. Zsigulics, P. Angyal, B. B. Mészáros, Dr. Sz. Varga, Dr. T. Soós
Organocatalysis Research Group
Institute of Organic Chemistry, HUN-REN Research Centre for Natural Sciences
2. Magyar tudósok krt., H-1117 Budapest, Hungary
E-mail: varga.szilard@ttk.hu, soos.tibor@ttk.hu

[b] B. Zsigulics, P. Angyal, B. B. Mészáros
Hevesy György PhD School of Chemistry
Eötvös Loránd University
1/a Pázmány Péter sétány, H-1117 Budapest, Hungary

[c] B. B. Mészáros, Dr. J. Daru
Department of Chemistry
Eötvös Loránd University
1/a Pázmány Péter sétány, H-1117 Budapest, Hungary
E-mail: janos.daru@ttk.elte.hu

Supporting information for this article is given via a link at the end of the document.

Abstract: A short, bioinspired, and enantioselective synthesis of (–)-hunterine A, an odd 6/7/6/6/5 pentacyclic natural product, is described. The key step in the synthesis of this daunting structure is the 6-exo selective epoxide ring-opening reaction, which is interwoven with a deconstructive step of the indolenine part to create the unusual 7-membered azepine bridge motif. Our work also reveals the possible mechanism and stereochemical prerequisite of this unique skeletal rearrangement, which provides a vantage point for understanding how (–)-hunterine A is likely to be generated in nature.

Divergent biosynthesis is a fundamental strategy present in nature, which facilitates chemical diversity in the generation of biologically active natural products.[1] Unveiling different chemical facets of this strategy is particularly important, as it also provides a rich source of inspiration for the discovery of novel strategies and tactics in chemical synthesis.[2] Guided by this approach, we have been drawn to a distinct subclass of aspidosperma alkaloids that possess a C-20 or C-21 oxidized ethyl side chain. With this subtle yet remarkable structural modification, nature has utilized a molecular springboard to a diverse array of more complex alkaloids in a few steps, including pleiocarpine-refractine alkaloids (Figure 1a). This divergent biosynthetic strategy has also been successfully translated into divergent synthetic approaches, as several streamlined syntheses of these structurally unique alkaloids have been reported by us[3] and others[4]. While these advances have greatly expanded the synthetic accessibility of these topologically different aspidosperman derivatives, the elaboration of these complex natural products typically occurs via simple C-C or C-O bond formation, without any rearrangement of the heterocyclic ring[5]. Herein, we describe a further extension of this molecular springboard strategy toward coupled framework reorganization and report the bioinspired total synthesis of (–)-hunterine A (**1**) (Figure 1b).

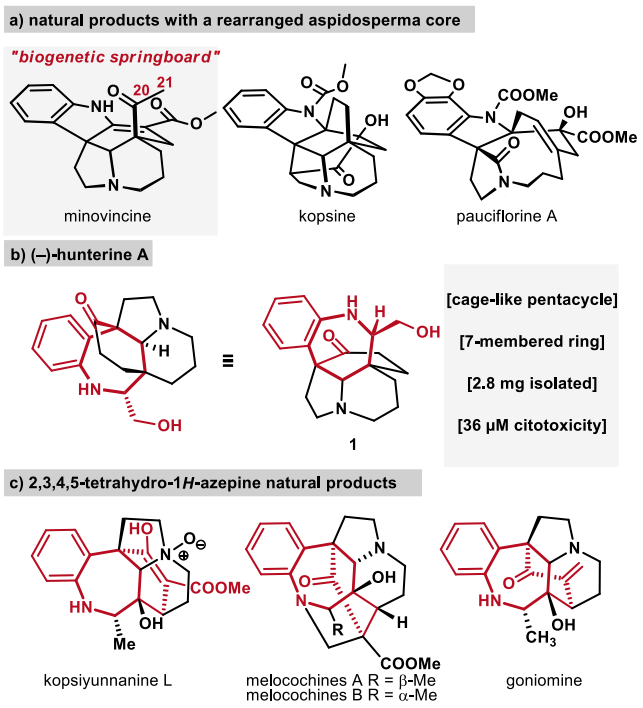

Figure 1. Introduction to (–)-hunterine A and related natural products.

(–)-Hunterine A (**1**), isolated from *Hunteria zeylanica* by Zhang, Ye, Zhang et al. in 2019,[6] is a member of a structurally distinct class of terpenoid indole alkaloids featuring an unusual 6/7/6/6/5 pentacyclic ring system with a rare 7-membered 2,3,4,5-tetrahydro-1*H*-azepine bridge motif (Figure 1c).[7] The limited access to this alkaloid, 2.8 mg of which was isolated from 9.5 kg of dried leaves, allowed only preliminary, but still promising assessment of its biological activity; (–)-hunterine A (**1**) showed

moderate cytotoxic activity against HepG2 human cancer cell lines.[6] In addition, Zhang, Ye, Zhang et al. proposed a plausible biogenetic pathway that can be traced back to the indole natural product tuboxenine (**2**), which is co-isolated with **1**. Thus, it has been suggested that after the ring opening of the putative intermediate **2**, epoxidation occurs at the C-20 and C-21 positions, and the resulting reactive intermediate **3** is rearranged to **1** (Figure 2a).

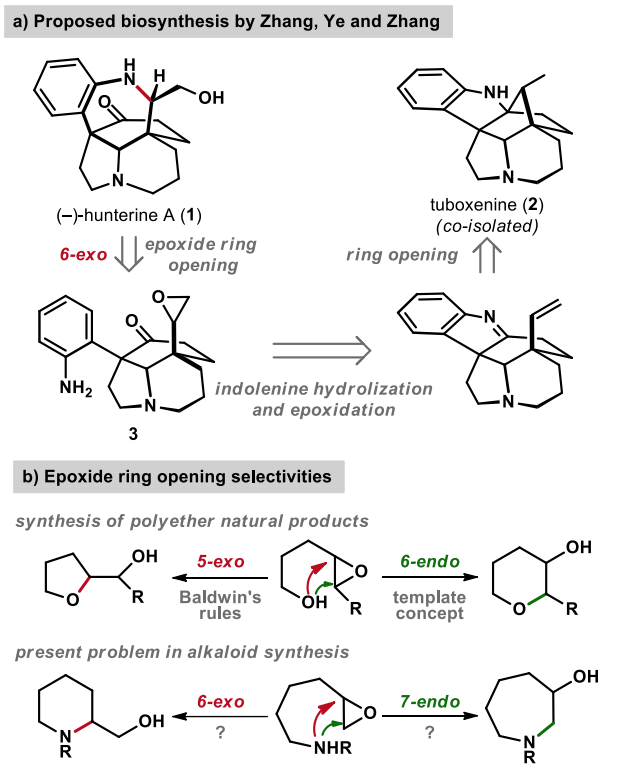

Figure 2. a) Introduction to the proposed biosynthesis of (–)-hunterine A (**1**) **b)** the regioselectivities observed in related state-of-the-art epoxide transformations.

Stimulated by the proposed biogenetic pathway and the synthetic challenges of constructing the intricate cage-like structure of (–)-hunterine A, coupled with the low isolation efficiency and promising bioactivity of the monoterpene indole alkaloid **1**, we embarked on the bioinspired total synthesis of (–)-hunterine A (**1**).[8] In addition to underpinning the biogenetic pathway and successfully implementing a bioinspired synthetic strategy, we also aimed to unravel the chemical facets of the critical epoxide ring-opening reaction of the proposed biogenetic pathway. More specifically, we were curious to know what factor drives the more encumbered 6-exo ring opening instead of the alternative 7-endo process. Interestingly, analogous ring-opening reactions have been broadly utilized in nature for the assembly of various polyether natural products (Figure 2b).[9] To date, however, all existing synthetic cascades have required a directing group at the epoxide functionality to ensure high selectivity in 6-endo over 5-exo product formation.[10] Thus, if the epoxide opening reaction is indeed used in the biosynthesis of (–)-hunterine A (**1**), it was unclear at the beginning of our total synthesis project how the preference for exclusive selectivity is ensured, e.g., by enzymatic vs. template control. In addition, non-productive hydrolytic events (i.e., hydrolysis of the epoxide to a diol) and cationic rearrangement of the epoxide (i.e., Wagner–Meerwein rearrangement) are likely to be competitive pathways,[11] so achieving the desired ring opening and deconstructive rearrangement may require further mechanistic understanding and extensive experimentation.

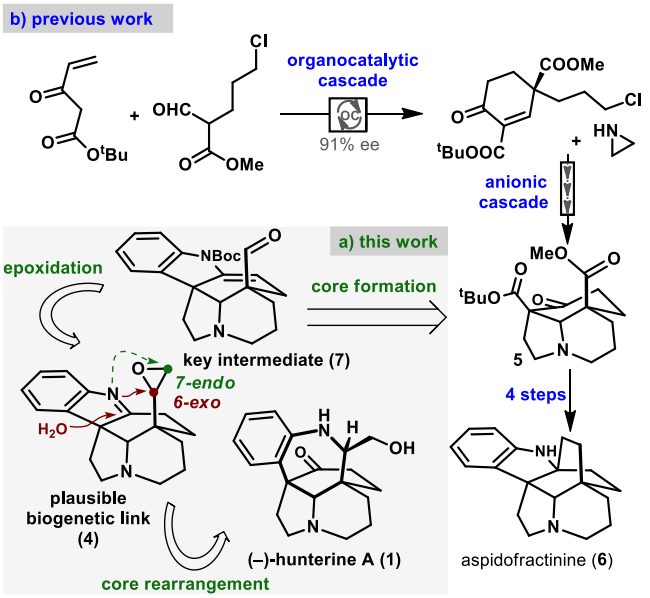

Figure 3. Our recent synthetic design to furnish (–)-hunterine A (**1**) building on our previous work on aspidosperma alkaloids.

With the joint aims of addressing this selectivity issue and accelerating the synthesis of (–)-hunterine A (**1**) via a molecular springboard strategy, we focused our efforts on a directing-group-free approach that utilizes an easily accessible C-20 oxidized aspidosperma building block. Therefore, as a working hypothesis, we postulated that the aspidosperma indolenine epoxide **4** could be the possible biogenetic and synthetic link between aspidospermans and (–)-hunterine A (**1**) (Figure 3a).

Bolstered by the realization that the synthetic route can be reduced to the synthesis of indolenine epoxide **4** and its ring opening to (–)-hunterine A (**1**), the envisaged bioinspired approach was guided by our previous experience[3] with the modified Stork's tricyclic ketone **5** (Figure 3b). This advanced intermediate, easily available at a multidecagram-scale in an organocatalytic cascade, has served as a branching point for a number of topologically different indole alkaloids (e.g., aspidofractinine (**6**)) and has also served as the starting point for the present synthetic campaign. Accordingly, as a first foray, we sought to develop the multigram-scale synthesis of the aldehyde derivative **7** as a key intermediate (Figure 4a). Thus, the previously developed diester **8** was exposed to acidic conditions to yield tricycle **9** via a sequence of selective hydrolysis and subsequent decarboxylation. The following Fischer indolization readily furnished indolenine **10** on a 7.0 g scale.[12] Then, the reduction-sensitive indolenine functionality was protected as Boc-enamine **11** after deprotonation of **10** with LDA. This set the stage for the partial reduction of the ester functionality in two redox steps (DIBAL-H, then DMP).[13] With multigram quantities of the key aldehyde intermediate **7** in hand, the next tactic was to reach the required epoxide to produce the biosynthetic precursor indolenine

epoxide **4**. First, the proposed biogenetic route was followed, so the alkene epoxidation pathway[14] was explored. Deprotection of the *tert*-butoxycarbonyl group using TFA into **12** and subsequent Wittig reaction[13] of the aldehyde group readily furnished alkene **13**. However, despite screening several oxidative protocols (for more details, see the Supporting Information), no conditions were found to bring about the desired transformation. This setback prompted consideration of an alternative route to access indolenine epoxide **4**. Thus, C1 homologation of aldehyde **12** with nucleophilic carbenoids[15] was investigated. Gratifyingly, under cryogenic conditions, the lithium carbenoid gave **4-epi-1** epoxide as a single diastereomer.[16] This advance paved the way for accomplishing the critical ring-opening steps, however, we were unable to detect the formation of even trace amounts of (–)-hunterine A (**1**) after subjecting **4-epi-1** to various hydrolytic/acidic conditions. Nevertheless, we were intrigued by the observed isomeric product **14** of these hydrolytic events (i.e., in aq. H_2SO_4). Structural analysis of this isomeric product suggested that **14** did form in a 7-endo ring opening process and the configuration of the epoxide moiety at the C-20 position was the opposite of that required for (–)-hunterine A (**1**) formation. The formation of this isomeric product **14** also implied that the 6-exo vs. 7-endo selectivity appears to be under substrate control, which may shift toward 6-exo selectivity when the epoxide ring configuration is reversed. Accordingly, we turned our attention to the preparation of the alternative, diastereomeric protected epoxide indolenine **15-epi-2** to complete the bioinspired total synthesis of (–)-hunterine A (**1**). After much experimentation, we finally identified a method using the Corey-Chaykovsky reaction[17] that could provide the desired stereoisomer, but only as a non-separable 1:2 diastereomeric mixture, and this method could be readily scaled up to the gram scale. At this juncture, we proceeded to convert **15** into (–)-hunterine A (**1**) in a cascade process that included the critical 6-exo epoxide ring opening and the deconstruction of the indolenine moiety to a bridged azepine. To our delight, after subjecting the diastereomeric mixture of Boc-protected indolenine epoxides **15** to aqueous sulfuric acid under biphasic conditions (dichloromethane/water), (–)-hunterine A (**1**) was formed in acceptable amounts via a sequence consisting of deprotection/hydration/epoxide ring opening/ring expansion steps. It is also worth noting that our study revealed a rare example of a diastereodivergent transformation from the same aspidosperma core, resulting in the formation of structurally strikingly different rearranged products. Finally, we raise the possibility that if the epoxidation of the putative intermediate is not completely stereoselective in the biogenetic route, the isolated 7-endo product **14** may be a yet unknown “iso-hunterine A” natural product.[18]

Spurred on the successful accomplishment of the bioinspired total synthesis of (–)-hunterine A (**1**), we were keen to gain further mechanistic insights into this bioinspired skeletal rearrangement. To simplify our combined experimental and theoretical mechanistic studies and confirm certain intermediates of the developed cascade process, we synthesized (for more details, see the Supporting Information) **4-epi-1**, **4-epi-2**, and **16** (as a mixture of epimers **16-epi-1** and **16-epi-2**) and subjected them to the same acidic conditions as above. As expected, **4-epi-1** exclusively gave “iso-hunterine A” (**14**), while **4-epi-2** furnished (–)-hunterine A (**1**) as the sole product. Additionally, the reaction of **16** was found to result in the formation of both products (for more details, see the Supporting Information). These results clearly reinforced the decisive role of C-20 stereochemistry in the diastereodivergent[19] formation of 6- or 7-membered rings and indicated that both **4-epi-2** and **16-epi-2** are possible productive intermediates of (–)-hunterine A synthesis. Then, we endeavored to validate the pathways leading to “iso-hunterine A” (**14**) and (–)-hunterine A (**1**) using computational methods (for more details see the Supporting Information). Since the hydrolytic ring opening of the **4-epi-1/2** reactions occurred in aqueous media using an excess of sulfuric acid, we assumed that the doubly protonated species **A1-*S*** is present in the initial state of these reactions. This intermediate undergoes a water addition from the more accessible convex face (Figure 4b) through a relatively low barrier of 14.7 kcal/mol (via **[A1-*S*]‡**), giving hemiaminal **A2-*S***, the branching point for two competing pathways to give the same final product.

First, the previously suggested biogenetic path was evaluated. In this route (**path A**, Figure 4b, red), the ring opening of the hemiaminal functionality through **[A2-*S*]‡** (25.0 kcal/mol) gives aniline **A3-*S*,** which is a high-lying intermediate (12.9 kcal/mol), then, the ring closure of the aniline nitrogen on the epoxide yields the doubly protonated (–)-hunterine A (**PROD**). This latter, rate-limiting step is characterized by a prohibitively high activation energy (33.6 kcal/mol, via **[A3-*S*]‡**). However, if the 6-exo-type epoxide ring opening takes place first from **A2-*S*** (**path B,** green), the barrier height of this rate-determining step is only 23.6 kcal/mol (via **[B2-*S*]‡**), leading to a stable intermediate **B3-*S***. This intermediate then undergoes ring opening through a 14.3 kcal/mol relative free energy barrier (0.4 kcal/mol, via **[B3-*S*]‡**) to give **PROD**, although, this step is endergonic by 4.0 kcal/mol. As we further explored this thermodynamic equilibrium, we found that (–)-hunterine A (**1**) is thermodynamically more stable both in neutral aqueous and in organic media than **B3-*S***, which is preferred only when both nitrogens are protonated in a highly acidic media (for more details see the Supporting Information). This mechanistic scenario suggests that the hydrolysis of the indolenine hemiacetal to the azepine ring is the last step of this cascade, i.e., the previously hypothesized biogenetic "aniline pathway" (Figure 4b, red) is a less likely route. Subsequently, we aimed to understand the distinct 6-exo and 7-endo reactivities of **4-epi-1** and **4-epi-2,** which ultimately resulted in highly selective diastereodivergent routes (Figure 5a). The (–)-hunterine A-forming hemiaminal intermediate **A2-*S*** needs to overcome a relative barrier of 24.2 kcal/mol (via **[B2-*S*]‡**) in the case of a 6-exo epoxide ring opening, but significantly higher activation energy is required (29.6 kcal/mol, via **[C2-*S*]‡**) to induce 7-endo epoxide ring opening, although the 7-endo product is thermodynamically more stable. On the other hand, the diastereomeric **A2-*R*** has a kinetic preference toward 7-endo epoxide ring opening (17.5 kcal/mol, via **[C2-*R*]‡**) to give the “iso-hunterine” product **C3-*R*** (-23.9 kcal/mol).

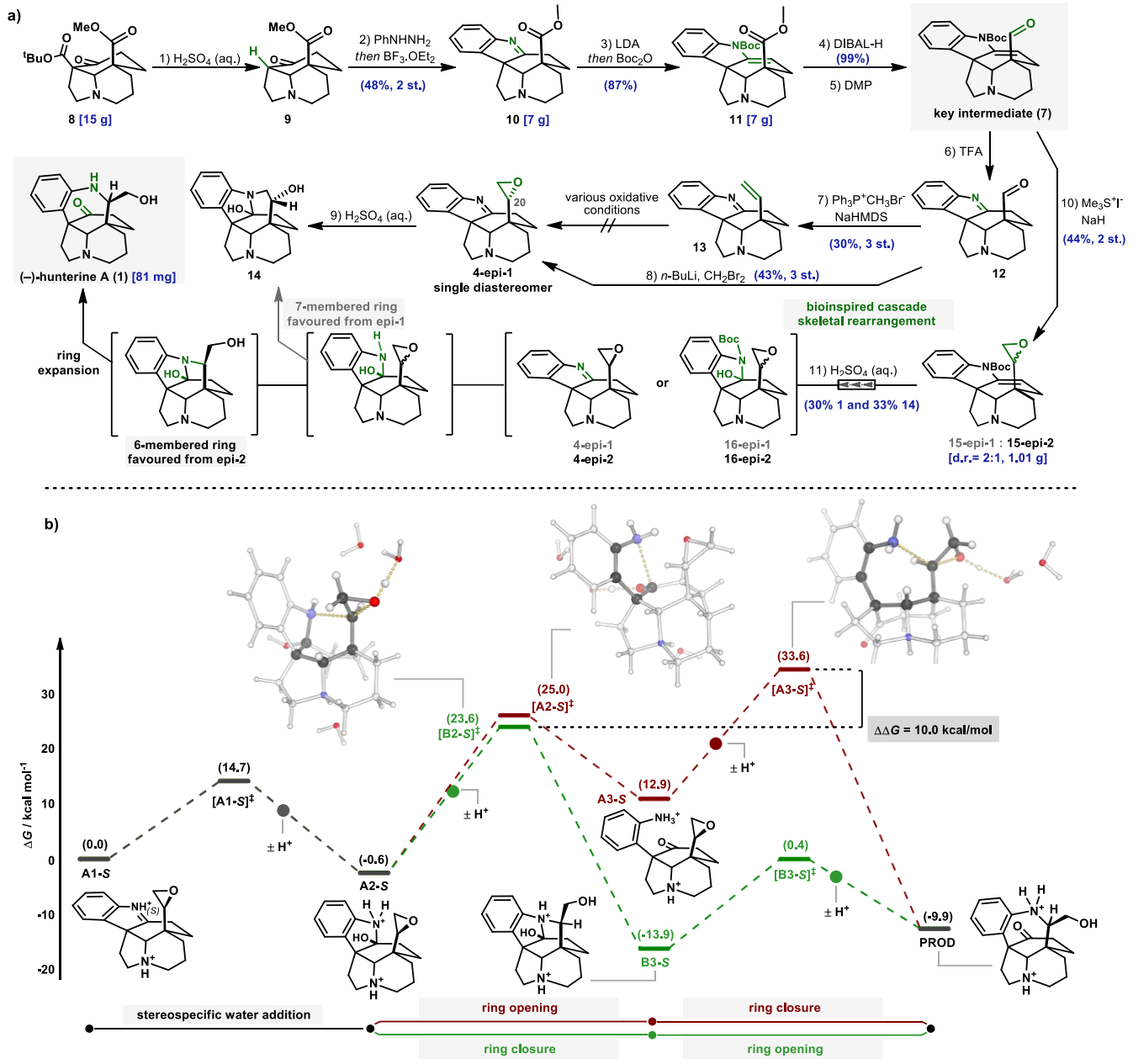

Figure 4. a) The total synthesis of (–)-hunterine A featuring a bioinspired cascade skeletal rearrangement. Reagents and conditions: 1) 50 V/V% H_2SO_4 (aq.), 1,4-dioxane, 25 °C; 2) $PhNHNH_2$ (1.05 eq.) *then* 10 V/V% $BF_3{\cdot}OEt_2$ (MeOH), 70 °C; 3) LDA (4.85 eq.), THF, -78 °C *then* addition of Boc_2O (5.0 eq.) in THF, -78 °C; 4) DIBAL-H (2.0 eq.), toluene, -78 °C; 5) DMP (2.0 eq.), CH_2Cl_2, 0 to 25 °C; 6) TFA (60 eq.), CH_2Cl_2, 0 to 25 °C; 7) $Ph_3P^+CH_3Br^-$ (10.0 eq.), NaHMDS (9.0 eq.), THF, -45 °C, *then* addition of **12** in THF, -45 to 0 °C; 8) CH_2Br_2 (1.2 eq.), THF, 25 °C, *then* *n*-BuLi in THF (1.05 eq.), -78 to 25 °C; 9) 10 V/V% H_2SO_4 (aq.), CH_2Cl_2, 25 °C; 10) $Me_3^+SI^-$ (4.0 eq.), NaH (4.0 eq.), DMSO, 25 °C *then* addition of **7** in DMSO, 15 to 25 °C; 11) 10 V/V% H_2SO_4 (aq.), CH_2Cl_2, 25 °C. THF= tetrahydrofuran, LDA=lithium diisopropylamide, Boc_2O=di-tert-butyl dicarbonate, DIBAL-H=diisobutylaluminum hydride, DMP=Dess–Martin periodinane, TFA=trifluoroacetic acid, NaHMDS=sodium bis(trimethylsilyl)amide, DMSO=dimethyl sulfoxide. **b)** Free energy diagram of possible mechanistic routes (A and B, depicted with red and green, respectively, states shared by both pathways shown in black) and 3D structures of transition states (carbon: black, hydrogen: white, nitrogen: blue, oxygen: red), where suspector atoms are depicted with smaller sizes (white for carbon).

As seen above, we faced a quandary that although the formation of the 7-membered-ringed endo products is thermodynamically favored for both diastereomers, the kinetics override the 7-endo preference in the case of *S*-epoxide. Furthermore, both ring sizes are allowed according to Baldwin's rules,[20] therefore, we suggested that the rigid aspidosperma skeleton governs the selectivity. To test this hypothesis, we performed calculations on disconnected model reactions with an aniline derivative having similar electronic properties but no ring strain by construction (Figure 5b). In these intermolecular models, the attack on the terminal carbon atom is favored, regardless of the epoxide configuration. However, if the ring closure occurs inside the rigid intramolecular framework, the activation energy increases, especially for the *S*-epoxide (Figure 5b). This implies that the spatial orientation is unfavorable in the *S*-epoxide, particularly in **[C2-*S*]‡** (Figure 5c), suppressing the 7-membered ring formation. Thus, the ring strain results in an inverse selectivity, and forces the exclusive formation of the 6-membered ring leading to (-)-hunterine A in the subsequent steps.

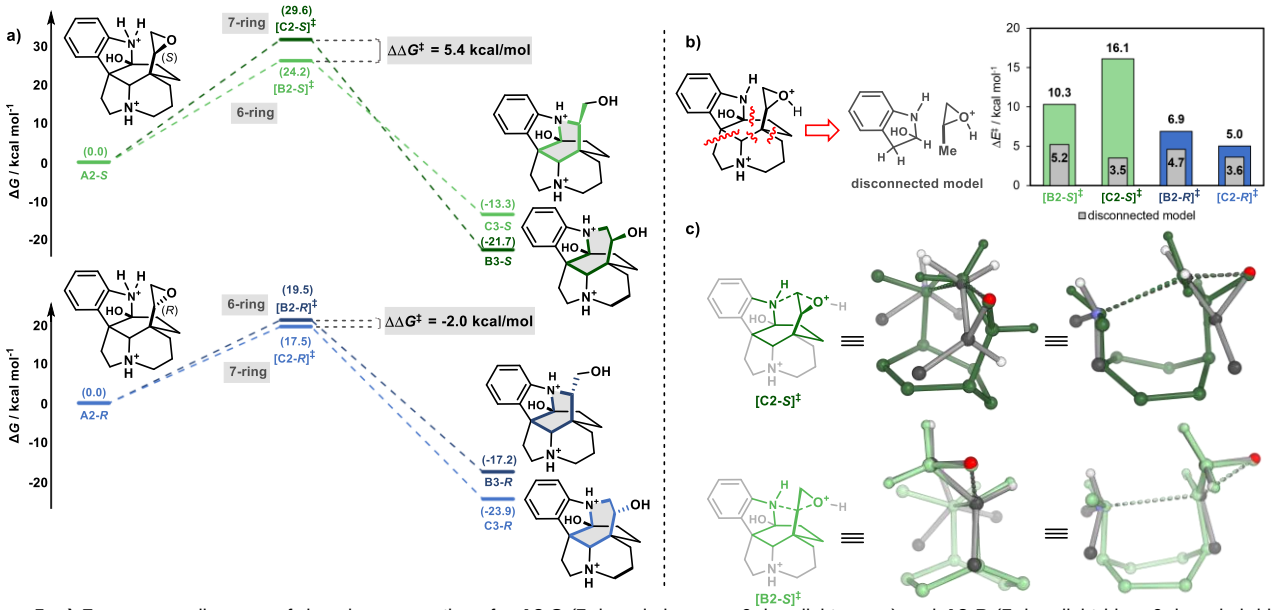

Figure 5. a) Free energy diagrams of ring closure reactions for **A2-*S*** (7-ring: dark green, 6-ring: light green) and **A2-*R*** (7-ring: light blue, 6-ring: dark blue). **b)** Disconnected models, and comparison of their activation energies with the original systems **c)** Overimposed 3D structures of **[C2-*S*]‡** (dark green) and **[B2-*S*]‡** (light green) and the corresponding model systems (carbon: black, hydrogen: white, nitrogen: blue, oxygen: red), where only atoms of a six-membered ring and those involved in the reaction are shown for simplicity (also highlighted on the 2D chemical structures).

Finally, one of the logical consequences of our studies has prompted us to do further research. As our synthetic and mechanistic work has clearly shown that (–)-hunterine A (**1**) can be generated from the indolenine precursor **4-epi-2** via a non-enzymatic acidic rearrangement, we hypothesized that (–)-hunterine A (**1**) might actually be an isolation artifact[21]. Thus, **4** was subjected to acidic conditions (HCl (aq.), pH=3) similar to those used by Zhang during the isolation procedure, however, no formation of (–)-hunterine A (**1**) was observed (for more details, see the Supporting Information). This observation suggests that (–)-hunterine A (**1**) is indeed a natural product of the *Hunteria zeylanica* plant.

In conclusion, we accomplished the bioinspired total synthesis of (–)-hunterine A (**1**). The described assembly provides evidence for the proposed biogenetic pathway, adding further and fundamental mechanistic details about the epoxide ring opening and the interwoven indolenine deconstruction. In addition, the rare phenomenon of diastereodivergent ring opening of the epoxide was revealed. Thus, the C-20 stereochemistry was found to be decisive in the outcome of the key rearrangement that ultimately leads to different ring systems due to a significant ring-strain effect in one of the diastereomers. Accordingly, the cage-like aspidosperma core prevents the 7-endo pathway and governs the reaction towards the 6-exo route. We believe that the knowledge detailed here will be well applicable to the synthesis of similar unconventional cage-like structures and encourage further exploration thereof.

Supporting Information

The authors have cited additional references within the Supporting Information.[3a, 22 - 31]

Acknowledgements

Financial support provided by the grants NKFIH FK138300, FK147031 and K147280 are gratefully acknowledged. Project no. 1015948 has been implemented with the support provided by the Ministry of Culture and Innovation of Hungary from the National Research, Development and Innovation Fund, financed under the KDP-2020 funding Scheme (P. A.). Supported by the ÚNKP-22-2, and ÚNKP-23-3 New National Excellence Programs and the DKOP-23 Doctoral Excellence Program of the Ministry for Culture and Innovation from the source of the National Research, Development and Innovation Fund (B. B. M.). The authors thank the Servier Research Institute of Medicinal Chemistry for the HRMS measurements.

[1] a) Q. Wei, H.-C. Zeng, Y. Zou, *ACS Catal.* **2021**, *11*, 948–957.; b) Z.-R. Li, J. Li, J.-P. Gu, J. Y. H. Lai, B. M. Duggan, W.-P. Zhang, Z.-L. Li, Y.-X. Li, R.-B. Tong, Y. Xu, D.-H. Lin, B. S. Moore, P.-Y. Qian, *Nat. Chem. Biol.* **2016**, *12*, 773–775.

[2] a) H. M. S. Haley, S. E. Payer, S. M. Papidocha, S. Clemens, J. Nyenhuis, R. Sarpong, *J. Am. Chem. Soc.* **2021**, *143*, 4732–4740.; b) V. C. Fäseke, F. C. Raps, C. Sparr, *Angew. Chem. Int. Ed.* **2020**, *59*, 6975–6983.; c) J. C. P. Reyes, D. Romo, *Angew. Chem. Int. Ed.* **2012**, *51*, 6870–6873.

[3] a) S. Varga, P. Angyal, G. Martin, O. Egyed, T. Holczbauer, T. Soós, *Angew. Chem. Int. Ed.* **2020**, *59*, 13547–13551.; b) G. Martin, P. Angyal, O. Egyed, S. Varga, T. Soós, *Org. Lett.* **2020**, *22*, 4675–4679.

[4] a) K. L. White, M. Movassaghi, *J. Am. Chem. Soc.* **2016**, *138*, 11383–11389.; b) B. N. Laforteza, M. Pickworth, D. W. C. Macmillan, *Angew. Chem. Int. Ed.* **2013**, *52*, 11269–11272.; c) M. E. Kuehne, Y. L. Li, *Org. Lett.* **1999**, *1*, 1749–1750.

[5] an example for the destructive skeletal rearrangement of the terpene core: ref 4a

[6] J. Zhang, Z.-W. Liu, Y.-L. Ao, L.-J. Hu, C.-J. Wei, Q.-H. Zhang, M.-F. Yuan, Y. Wang, Q.-W. Zhang, W.-C. Ye, X.-Q. Zhang, *J. Org. Chem.* **2019**, *84*, 14892–14897.

[7] a) Y. Zhang, X. Ding, S. Shao, L.-L. Guo, Q. Zhao, X.-J. Hao, H.-P. He, *Org. Lett.* **2019**, *21*, 9272–9275.; b) *Tetrahedron* **2016**, *72*, 6692–6696.; c) A. Chiaroni, L. Randriambola, C. Riche, H. P. Husson, *J. Am. Chem. Soc.* **1980**, *102*, 5920–5921.

[8] During the preparation of this manuscript, Stoltz and co-workers reported the non-bioinspired total synthesis of (-)-hunterine A: E. F. Hicks, K. Inoue, B. M. Stoltz, *J. Am. Chem. Soc.* **2024**, *146*, 4340–4345.

[9] a) J. I. Bowen, L. Wang, M. P. Crump, C. L. Willis, *Org. Biomol. Chem.* **2022**, *20*, 1150–1175.; b) I. Vilotijevic, T. F. Jamison, *Mar. Drugs* **2010**, *8*, 763–809.

[10] selected example: I. Vilotijevic, T. F. Jamison, *Science* **2007**, *317*, 1189–1192.

[11] T. Feng, Y. Li, Y.-P. Liu, X.-H. Cai, Y.-Y. Wang, X.-D. Luo, *Org. Lett.* **2010**, *12*, 968–971.

[12] Slightly modified and upscaled versions of the previously reported procedures were used in these steps, see ref 3a

[13] H. Mizoguchi, H. Oikawa, H. Oguri, *Nat. Chem.* **2014**, *6*, 57–64.

[14] I. Carqueijeiro, S. Brown, K. Chung, T.-T. Dang, M. Walia, S. Besseau, T. Dugé de Bernonville, A. Oudin, A. Lanoue, K. Billet, T. Munsch, K. Koudounas, C. Melin, C. Godon, B. Razafimandimby, J.-O. de Craene, G. Glévarec, J. Marc, N. Giglioli-Guivarc'h, M. Clastre, B. St-Pierre, N. Papon, R. B. Andrade, S. E. O'Connor, V. Courdavault, *Plant Physiol.* **2018**, *177*, 1473–1486.

[15] L. Ielo, M. Miele, V. Pillari, L. Castoldi, V. Pace in Homologation Reactions: Reagents, Applications, and Mechanisms Vol. 1.(Ed.: Vittorio Pace), Wiley-VCH, **2023**, pp. 79-142.

[16] Unambiguous determination of the stereochemistry at C-20 was not possible at this point using standard NMR measurement techniques.

[17] a) L. Kürti, B. Czakó *Strategic Applications of Named Reactions in Organic Synthesis: Background and Detailed Mechanisms*. Elsevier, **2005**, pp. 102–103.; b) T. Saito, T. Suzuki, K. Takeuchi, T. Matsumoto, K. Suzuki, *Tetrahedron Lett.* **1997**, *38*, 3755–3758.

[18] B. E. Hetzler, D. Trauner, A. L. Lawrence, *Nat. Rev. Chem.* **2022**, *6*, 170–181.

[19] a) K. Pieper, R. Bleith, C. Köhler, R. Mika, A. Gansäuer, *Angew. Chem. Int. Ed.* **2024**, *63*, e202317525.; b) Y. Wang, X. Zhu, D. Pan, J. Jing, F. Wang, R. Mi, G. Huang, X. Li, *Nat. Commun.* **2023**, *14*, 4661.; e) J. Zhang, X. Huo, J. Xiao, L. Zhao, S. Ma, W. Zhang, *J. Am. Chem. Soc.* **2021**, *143*, 12622–12632. c) J. A. P. Maitland, J. A. Leitch, K. Yamazaki, K. E. Christensen, D. J. Cassar, T. A. Hamlin, D. J. Dixon, *Angew. Chem. Int. Ed.* **2021**, *60*, 24116–24123.; d) J. M. Müller, C. B. W. Stark, *Angew. Chem. Int. Ed.* **2016**, *55*, 4798–4802.

[20] K. Gilmore, R. K. Mohamed, I. V. Alabugin (2016). *Wiley Interdiscip. Rev. Comput. Mol. Sci.* **2016** *6*(5), 487-514.

[21] R. J. Capon, *Nat. Prod. Rep.* **2020**, *37*, 55–79.

[22] C. Bannwarth, S. Ehlert, S. Grimme, *J. Chem. Theory Comput.* **2019**, 15, 1652-1671.

[23] S. Ehlert. M. Stahn, S. Spicher, S. Grimme, *J. Chem. Theory Comput.* **2021**, 17, 4250–4261.

[24] S. Johannes, S. Kupfer, S. Gräfe. *Int. J. Quantum Chem.* **2021**, 121, e26390.

[25] J. G. Brandenburg, C. Bannwarth, A. Hansen, S. Grimme, *J. Chem. Phys.* **2018**, 148, 064104.

[26] F. Neese, *Wiley Interdiscip. Rev. Comput. Mol. Sci.* **2012**, 2, 73-78.

[27] V. Barone, M. Cossi, *J. Phys. Chem. A* **1998**, 102, 1995-2001.

[28] J.-D. Chai, M. Head-Gordon, *J. Chem. Phys.* **2009**, 131, 174105.

[29] F. Weigend, R. Ahlrichs, *Phys. Chem. Chem. Phys.* **2005**, 7, 3297-3305.

[30] H. Neugebauer, P. Pinski, S. Grimme, F. Neese, M. Bursch, *J. Chem. Theory Comput.* **2023**, 19, 7695-7703.

[31] Schrödinger, LLC, The PyMOL Molecular Graphics System, Version 1.8 **2015**.